Chapter 13

MODULATION OF RAT RADIAL OSTEOTOMY REPAIR USING ELECTROMAGNETIC CURRENT INDUCTION

P. Christel, G. Cerf, and A. A. Pilla

Introduction

THERE IS NOW LITTLE DOUBT that the periodic exposure of biological systems to low level pulsating current has a profound influence on the rate of tissue growth, repair, and maintenance. One major clinical application of this is the repair of some recalcitrant bone fractures (1). Guided by the historical speculation (2) that electrical activity is in some way associated with all cell and tissue regulation and/or function, it was proposed that dynamic electrochemical phenomena at cell surfaces and junctions could well constitute a general class of processes by which cellular control is expressed (3-5). Thus, simple changes in ionic microenvironment can influence the rate of cell differentiation and even redirect its developmental pathway (6-9). Changes in the chemical (including ionic) microenvironment caused by the faradaic (electrolysis processes occurring when DC current is passed through implanted electrodes can elicit osteochondrogenesis (10-12), bacteriostasis (13), and cellular dedifferentiation (7-9). The rate of cellular processes, such as DNA synthesis, can be increased by modification of the electrical characteristics of the cell/tissue culture vessel interface, caused by the application of high voltage via electrostatic coupling (14). The application of radiofrequency electrical signals, amplitude modulated at brain wave frequencies (6-20 Hz), influences Ca^{++} uptake in isolated cerebral tissue (21). Modification of the structure of cell/tissue junctions by mechanical means can modulate osteochondrogenesis (15). In fact, it is the latter phenomenon, which was empirically associated with the observation of strain generated potentials (16, 17) and the established piezoelectric properties of biopolymers (18, 19), such as bone collagen, that has stimulated the recent interest in electrical modification of bone repair. Following early pioneering reports, it has been clinically demonstrated that recalcitrant bone fractures can be healed using both D.C. and pulsating currents using implanted electrodes. It is evident that this modality of current injection results in electrolysis or faradaic effects that must modify the chemical composition of the extracellular medium. This approach involves both electrical and (primarily) chemical perturbations.

The proposal that, in all of the above, the unifying or common processes are electrochemical in nature has been tested by the formulation of the electrochemical information transfer concept (3). For this it was envisaged that the structure of biological membranes could readily lead to the consideration that potential (or charge) dependent processes, such as specific binding (adsorption) and/or membrane mass transport, can be key steps in regulation and can thus be kinetically modulated. The suggestion, therefore, is that if an appropriate real time coupling to the kinetics of these proposed regulatory electrochemical processes can be achieved, a net change in cell and/or tissue function may result. This has led to the development of a noninvasive technique (1) in which pulsating current induced electromagnetically is applied to the fracture site via external coils. The characteristics of the induced current were chosen to electrically couple to electrochemical cell surface phenomena involving, for example, ion binding and transport. The objective is to modulate the activity of membrane-bound enzymes or similar structures that may be involved in cell regulation. This study is specifically designed to assess the applicability of this approach to the in vivo process of callus formation of a fresh radial osteotomy in the rat. Three basic current waveform types were employed in order to provide a quantitative correlation between the kinetic characteristics of the waveform-cell surface process and the rate of mechanical evolution of fresh fracture repair.

Experimental

Outbred female Sprague Dawley rats weighing between 250 and 300 grams were employed in this study. Under general anesthesia (4%, 1cc/100g, chloral hydrate, intraperitoneal) both forelimbs were shaved and alcohol washed. A semisterile surgical procedure was employed. Each radius was exposed using a lateral approach between the carpi radialis and digitorum communis extensors. A transverse midshaft radial osteotomy was performed with a circular dental saw using serum saline irrigation. Care was taken to leave the ulna intact *and uninjured.* In this manner it could act as the major weight-bearing bone, minimizing a secondary displacement of the radial osteotomy and eliminating the need for internal fixation. Skin and facia were closed using 5.0 catgut. Operating time for both limbs was essentially identical. A postoperative x-ray was taken to check the integrity of the ulna.

After recovery (24 hours) the animals were placed in Plexiglas® restraining cages as shown in Figure 13.1 for twelve hours per day during thirteen days (14 days postoperative). All cages were mounted between two facing circular electrical coils 18 cm in diameter. All coils were 7 cm apart. These dimensions were dictated by the desire to obtain a spatially homogeneous time varying magnetic field at the fracture site. This has been found to be
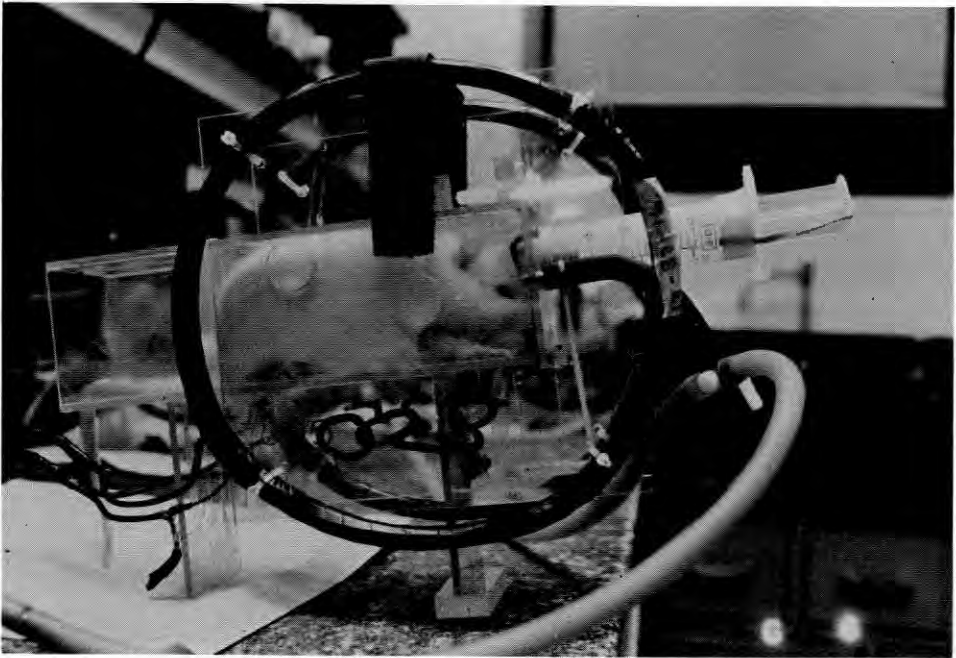
Figure 13-1. Photograph of the experimental coils utilized in this study. The rat is restrained in the plastic cage for twelve hours per day and is provided with food via the syringe normal to the front panel and water via a standard pressure activated nipple. The coils are powered to obtain the waveform configurations shown in Figure 13-2.

able to provide a relatively constant spatial distribution of current in the tissue (22, 23). Both active and control animals were identically restrained. For the remaining twelve hours all animals were placed, in groups of five, in a large cage where they were free roaming.

The three basic types of induced current waveforms employed are shown in Figure 13-2. All waveshapes exist as indicated in homogeneous conducting media (e.g. physiological saline) but will be modified in the presence of the electrical impedance of a cell membrane (20). Of importance to this study are the bipolar nature of the waveforms and their application in the periodic single pulse or pulse burst modality. The basic pulse parameters (Table 13-1) were chosen for efficient coupling to the kinetics of the class of cell surface processes anticipated as the most likely receptors for the weak currents employed. This approach allowed the prediction of the essential waveform characteristics of pulse width (τ_1, Fig. 13-2) and repetition rate (τ_5, Fig. 13-2). In addition, the general properties of electrochemical surface processes were used to approximately define the average change in charge (i. e. current density) to cause sufficient alteration in the ionic boundary conditions for cell function. In this study the peak current density at the leading edge of each pulse (A, Fig. 13-2)

varied between 1 and 10 $\mu A/cm^2$ as calculated and measured (22) for a homogeneous distribution of cells in conducting media (using 40% cell density).

Because of the physical requirement that equal energy be present in both polarity portions of the induced voltage waveform, it is obvious that, if the kinetics of the electrochemical process fall within the primary pulse duration, it must exhibit irreversibility. In other words, the cell surface process is expected to be nonlinear, at least to a small degree. Under these conditions the opposite polarity portion (τ_2, Fig. 13-2) of the main waveform would be expected to modify the net change in charge achievable in the cell/tissue complex. It is for this reason that the signal configurations a, b, and c (Fig. 13-2) were employed in this study.
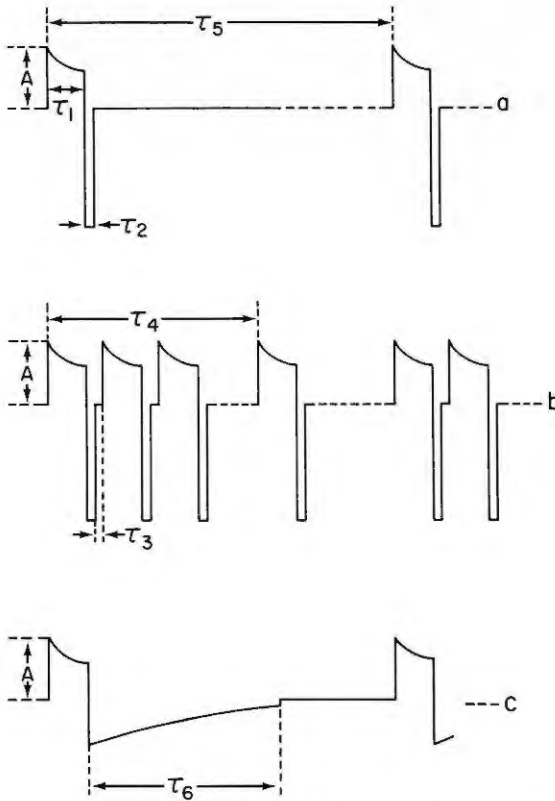

Figure 13-2. Schematic representation of the induced current waveforms employed in this study. The single repetitive pulses shown in "a" and "c" differed only by their opposite polarity configuration (τ_2 versus τ_6). The pulse burst waveform shown in "b" was configured as described in Table 13-I. The amplitude (A) utilized for calibration of the main polarity portion (τ_1) of each waveform is in arbitrary units referred to the probe coil described in the text.

In order to provide a quantitative correlation between signal configuration and the generalized cell surface electrochemical process, a model dependent frequency analysis has been developed (22). This takes into account all signal characteristics *and* the kinetics and reversibility of the surface response. Using this, correlations can be obtained both for wave form asymmetry and for burst and repetition rate changes. This will be illustrated below.

All electromagnetic devices were supplied by Electro-Biology, Inc. (Fairfield, New Jersey). They consisted of Helmholtz-aiding circular coils, 18 cm diameter, wound with forty to fifty turns of #16 B&S gauge copper magnet wire. The coils were powered with voltage pulses timed to achieve the induced voltage configurations shown in Figure 2. The amplitude designation A = 1 corresponds to a peak value of 15 mV for the main polarity waveform portion as measured with a 0.5 cm diameter probe coil wound with sixty-five turns of #36 B&S gauge copper magnet wire. This coil is calibrated to correspond to an induced voltage field of 1.5 mV/cm *for the perimeter of the probe coil.* The average magnetic field for A = 1 is 2 Gauss and that for A = 0.1 is 0.2 Gauss using the timing characteristics of the induced waveforms given in Table 13-I.

All animals were killed fourteen days postoperative with intraperitoneal injection of 4% chloral hydrate (2cc/100 g). Both radius and ulna were carefully dissected and immediately immersed in lactated Ringer's solution. Radiographs were then obtained in the anteroposterior and medial-lateral aspects. Only properly aligned fractures were retained for mechanical testing, thus assuring that the mechanical stress patterns affecting the evolution of osteotomy repair were as nearly identical as possible for each tested bone. Thus, osteotomies exhibiting angulation, medullary shift, and oblique line were discarded *before* mechanical test.

The tested osteotomies were subjected to a destructive tensile load using a MTS system fitted with a 500 N capacity load cell. The imposed deformation was 5 mm with a strain rate of 80 sec.$^{-1}$ Both ends of the bone pair

TABLE 13-I
INDUCED CURRENT WAVEFORMS FOR MODULATION OF
RAT RADIAL OSTEOTOMY REPAIR*

Waveform	$\tau_1(us)$	$\tau_2(us)$	$\tau_3(us)$	$\tau_4(ms)$	$\tau_5(Hz)$	$\tau_6(us)$	A
1	200	20	8	5	15	0	1
2	380	17	0	0	72	0	1
3	250	4	5	50	2	0	.1
4	380	0	0	0	72	4400	1
5	200	20	8	5	5	0	1

* Refer to Figure 13-2 for an explanation of all timing designations. Amplitude, A, refers to peak of main polarity portion of waveform and is in arbitrary units (text provides calibration details).
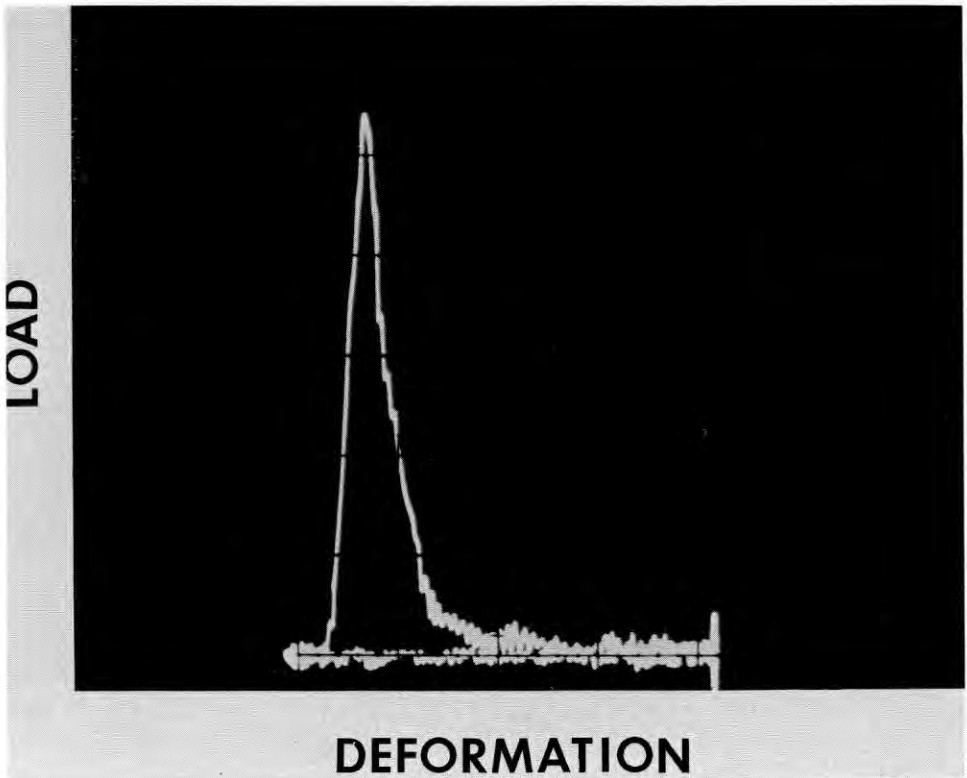
Figure 13-3. Photograph of a typical load deformation curve obtained by subjecting the radial osteotomy to a destructive tensile load (imposed deformation was 5 mm with a strain rate of 80 sec^{-1}). The peak of this curve provided the load values for comparison of treated and control osteotomies.

(radius plus ulna) were embedded in a special holder-fixture with dental acrylic cement. All embedding was carried out such that the long axis of the radius was in alignment with that of the rods connecting the fixture and the piston attachments. In this manner the bending component acting on the osteotomy site was minimized. Bones, holders, and rods were temporarily fixed together with a removable frame. After cement curing, the ulna was osteotomized with a dental saw, care being taken not to disturb the radius. The frame could then be removed and the destructive tensile test performed. Load-deformation curves were recorded using a memory oscilloscope (Tektronix 5103N). A typical curve is shown in Figure 13-3. The ultimate tensile strength is readily evaluated from the peak of these curves.

Using the above procedures, the effect of seven induced current signal configurations on ultimate tensile strength were examined. All signal and control groups were duplicated at several week intervals in order to ascertain the effect of possible evolving operative technique. Results were

anlyzed using the student T-test for an average of eleven well-aligned osteotomies per group.

Results and Discussion

The first phase of this study consisted of a survey of the signals shown in Figure 13-4. As can be seen, the basic waveform configurations shown in Figure 13-2 are included. Two of these signals (waveforms 1 and 4) have been employed in clinical studies involving the treatment of nonunions and pseudarthroses (1, 24, 25), wherein the observation is that configuration 1 more consistently achieves beneficial results. The objective in this phase, therefore, centered upon an assessment of the importance of opposite polarity parameters (waveforms 2 and 4) and on burst configuration (waveforms 1 and 3).

Examination of Figure 13-4 shows that the opposite polarity difference of waveform 4 as compared to waveform 2 rendered the former signal ineffective. When configuring signal 4 care was taken to modify only the opposite polarity width (τ^6 versus τ_2, Table 13-I and Fig. 13-2) of signal 2. In order to provide a quantitative assessment of this waveform difference
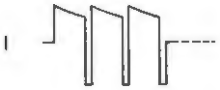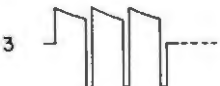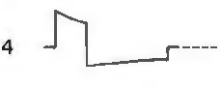

SIGNAL TYPE		% CHANGE vs CONTROL		
1	15 Hz 5 msec A=1	$+26.1 \pm 3.9$	$p < 0.001$	$N=17$
2	72 Hz 325/15 A=1	$+19.5 \pm 2.9$	$p < 0.001$	$N=15$
3	2 Hz 50 msec A=0.1	$+29.9 \pm 4.5$	$p < 0.001$	$N=17$
4	72 Hz 325/4500 A=1	$+8.5 \pm 1.3$	$p = 0.17$	$N=9$
5	5 Hz 5 msec A=1	-0.4 ± 0.06	$p > 0.9$	$N=13$

Figure 13-4. This is a table of results obtained using the waveforms designated (refer to Table 13-I for timing specifications). The percentage change refers to the difference in ultimate tensile strength between treated and control osteotomies. Note that actual waveform configuration appears critical in terms of modulation of the rate of mechanical evolution of the callus.

within the context of irreversible electrochemical cell surface phenomena, it is convenient to provide a kinetic description of the waveform-receptor combination. The details of this approach have been described elsewhere (22). Briefly, however, a frequency spectrum can be calculated using both waveform parameters and the kinetics (i.e. time constants) and reversibility of the cell surface process. An evaluation of the time constants of adsorption and transport pathways involved in the real-time response of living cell membranes has been reported for two cell systems (20, 26). Thus far, the most common transient current pathway across the cell membrane is functionally related to a specific binding (adsorption) process. Its value is situated between 10 and 100 μsec and appears to depend upon extracellular K^+ concentration for the human RBC (26). Utilization of these values for the range of relaxation times of the cell surface process and assigning a 10 percent nonlinearity (irreversibility) factor allows the frequency spectra shown in Figure 13-5 to be obtained. Here waveforms 1, 2, and 4 are compared. It can be seen that signals 1 and 2, which were nearly equally effective in terms of this mechanical readout, have similar amplitudes over the lower frequency range of the spectrum (<10 rad/sec). In comparison, signal 4 exhibits substantially lower amplitude over the same range. There
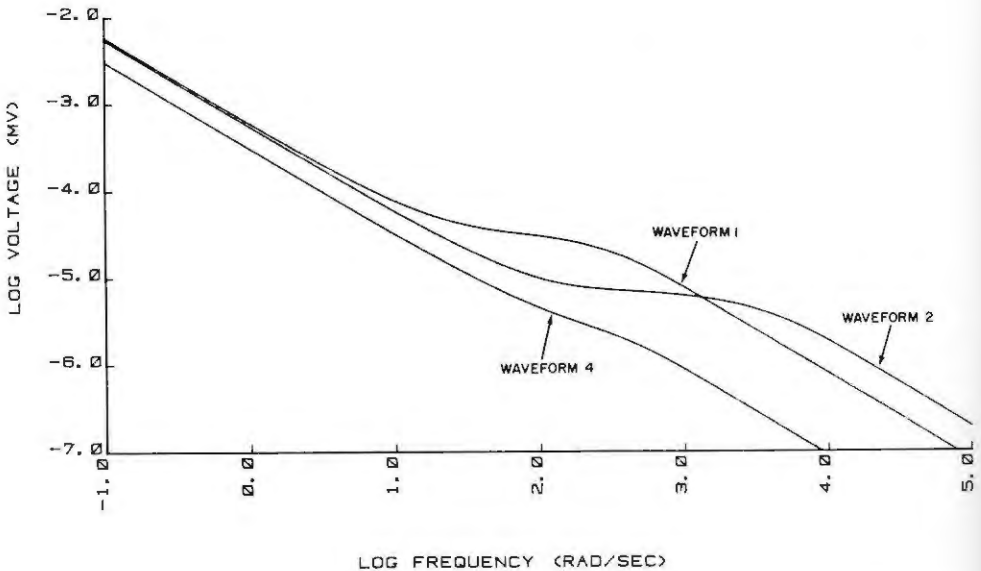

LOG FREQUENCY (RAD/SEC)

Figure 13-5. Electrochemical model dependent frequency spectra (via real axis Laplace transformation) for waveforms 1, 2, and 4. Of particular interest is the correlation of dose "amplitude" over the low frequency portion (<10 rad/sec) with the observed increase in ultimate tensile strength versus controls. Note that waveforms 1 and 2 were effective, while waveform 4 (which differed from the waveform 2 only in opposite polarity timing — see Table 13-I) was not. The voltage scale is arbitrary and useful only for signal comparison.

is no obvious trend over the remainder of the (higher) frequency range wherein the curves actually cross. At this point, therefore, it would appear that the major effect of increasing the duration of the opposite polarity portion of waveform 2 (to obtain waveform 4) is to significantly decrease the amplitude of the effective perturbation over the frequency range for which a quantitative correlation between signals 1 and 2 and mechanical read-out appears to exist. Note that the physical significance of "amplitude" in the frequency spectra described in this work depends upon the actual electrochemical process assumed to be the primary receptor of the induced current. For example, if specific ion binding at a membrane site is involved, then "amplitude" is directly related to the net increase (decrease) of the surface concentration of the ion in question.

The effect of pulse burst configuration can be seen by examination of Figure 13-4. Both waveforms 1 and 3 resulted in a nearly identical increase in ultimate tensile strength. Their model dependent frequency spectra are shown in Figure 13-6, where signal 2 is included for comparison. As can be seen, all three waveforms exhibit similar "amplitudes" over the low frequency portion (<10 rad/sec) of the spectrum. It is to be remembered that this quantitative correlation exists for signals having widely different real-time characteristics. For example, the peak amplitude of the main polarity portion of waveform 1 is ten times higher than that of waveform 3 (see Table 13-1). In addition, the duration of their opposite polarity portions differ by five times. The existence of a nearly identical correlation for these waveform configurations appears to indicate that it is primarily the kinetics and irreversibility factors that determine signal coupling efficiency. However, as has already been pointed out (23, 27), it may be important to take the potential dependence of electrochemical cell surface processes into account. In other words, if the combination of rate processes at the membrane is such that several waveform configurations can be created to obtain similar low frequency spectral "amplitudes," this does not preclude the possibility that several pathways may be current receivers. The question, therefore, is whether a very basic regulatory step is perturbed or whether many different cell surface regulatory processes, which are coupled to the various overall biochemical steps in the complexity of fracture repair, can act as the electrochemical receptors. In the latter case one likely possibility is that there are separate, but basic, regulatory steps as the stages of fracture repair progress (i.e. as the repair tissue differentiates). It is conceivable that all of these processes could possess similar potential dependence and kinetics *and* could have similar perturbation requirements. However, it is more probable that these requirements, as assessed by the "amplitude" versus frequency range of signal matching, can differ by at least one order of magnitude. One consequence of this is the distinct possibility of at least two net perturbation ranges over which some degree

of acceleration (or inhibition) of the biological end point (in this study —
mechanical) could be achieved. This has not yet been examined for radial
osteotomy repair but has been reported for Ca^{++} uptake (28). Here it was
demonstrated that the parameters of waveform 4 can be adjusted to obtain
essentially the same effect on Ca^{++} uptake in osteochondrogenic tissue,
while retaining the same basic waveform configuration (i.e. $\tau_1 \ll \tau_6$, Fig.
13-2).

In order to more carefully examine the "amplitude" (dosage) require-
ments for this fracture repair model and to eliminate variations in real-
time coupling to the cell process(es) supposed relevant, the waveforms
shown in Figure 13-7 were utilized. Here, the basic burst configuration of
waveform I was retained, only the burst repetition rate was varied. This
modification results in a progressive increase (as signal frequency rises) in
"amplitude" over only the low frequency portion of the model dependent
spectrum (see Fig. 13.8). In other words, variation of this waveform pa-
rameter allows the real-time electrical amplitude "seen" by the cell for each
pulse to remain constant *and,* in the frequency domain, results in dose
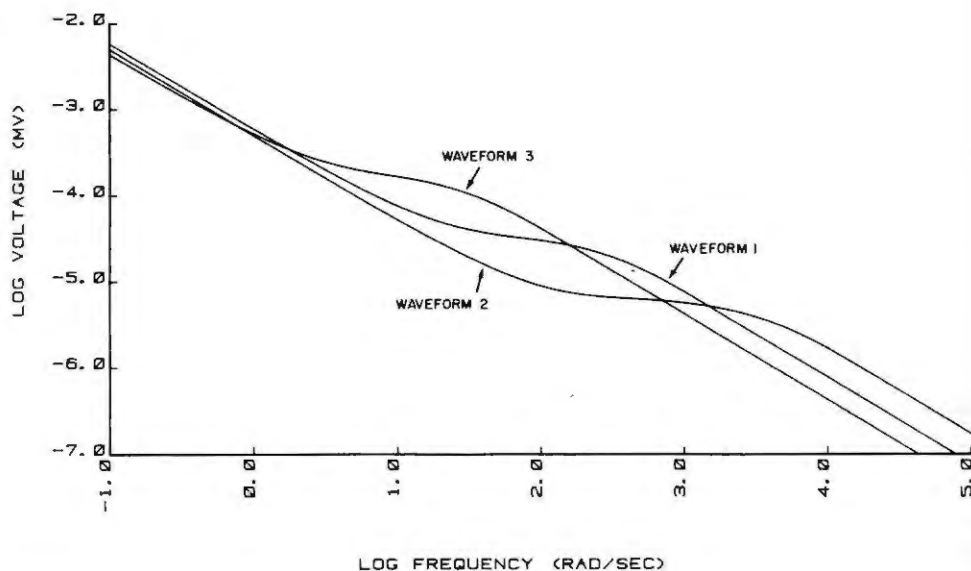"amplitude" variations only over the low frequency region.

Figure 13-6. Electrochemical model dependent frequency spectra showing effect of pulse
burst configuration (waveforms 1 and 3). Dose "amplitude" correlation versus observed
increase in ultimate tensile strength is evident over the low frequency portion (<10 rad/sec).
Evidence that a net perturbation is required is particularly shown by comparison with
waveform 2, which is a single pulse. The voltage scale is arbitrary and useful only for
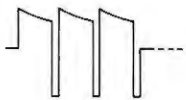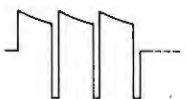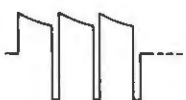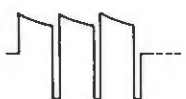comparison.

SIGNAL TYPE 5 MSEC BURST A=1	% CHANGE vs CONTROL		
5 Hz	− 0.4±0.06	p > 0.9	N=13
11 Hz	+ 21.5 ± 3.2	p = 0.005	N=17
15 Hz	+ 26.1 ± 3.9	p < 0.001	N=17
20 Hz	+ 7.1 ± 1.1	p = 0.223	N=10

Figure 13-7. This is a table of results showing the effect of repetition rate on the basic pulse burst signal (waveform 1). Timing characteristics are given in Table 13-I for this signal. Of particular note is the apparent existence of a dose "amplitude" window within which the net perturbation is sufficient to cause the observed increase in ultimate tensile strength.

As can be seen from Figure 13-7, waveform 1 repeating at 11 and 15 Hz significantly (and nearly identically) increased the ultimate tensile strength of rat radial osteotomies versus controls at fourteen days postoperative. Of even greater significance, however, is the result that repetition rates above (20 Hz) and below (5 Hz) this range had no effect on this mechanical property. This appears to indicate that there is a dose "amplitude" window to achieve the biological end point of this study. Interestingly, every in vitro and in vivo system thus far examined exhibits a similar window when model-dependent frequency domain correlation is carried out. Under the conditions of this waveform variation the results correspond to a remarkable degree with clinical observations for nonunion repair (1, 24, 25). Thus, "best" results are obtained when the combination of signal parameters are such that the dose "amplitude" falls within the values bracketed by the 11 and 15 Hz waveforms (see Fig. 13-8). As has been pointed out elsewhere (22, 27), this does not mean that this is the only dose "amplitude" window range. Even more importantly, it does not mean that a constant kinetic coupling is optimal. Thus, as the repair process progresses, it could be expected that the programmed application of waveforms configured to kinetically couple to cell surface processes, such that two or more dose "amplitude" windows are achieved, may result in significantly greater modulation of fracture healing.
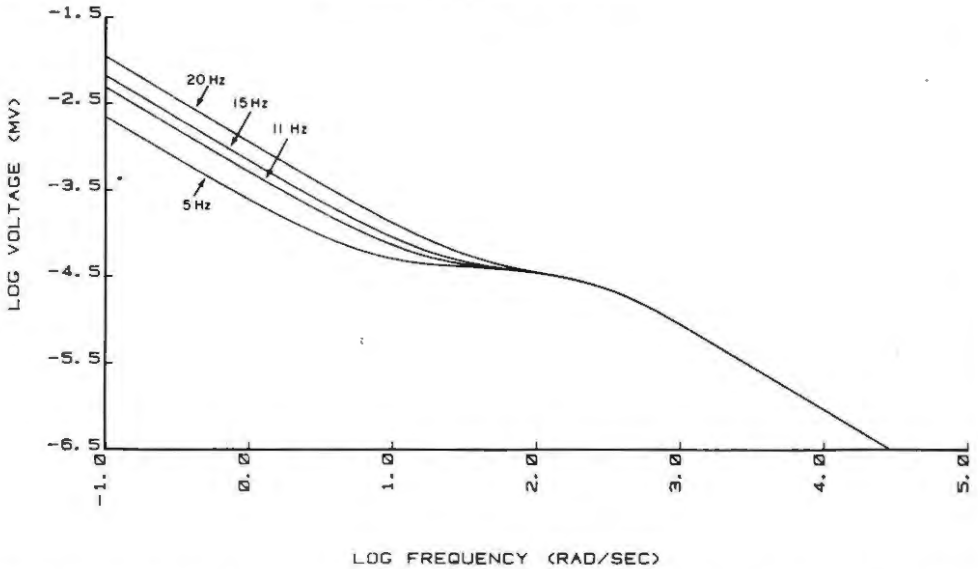
Figure 13-8. Real axis model dependent frequency spectra for the waveforms shown in Figure 13-7. The effect of repetition rate is seen only over the low frequency portion (<10 rad/sec) and provides strong indication that a net perturbation versus a cyclical perturbation) is required to achieve the observed biological effect. The voltage scale is arbitrary and is useful only for waveform comparison.

Conclusions

The results obtained in this study clearly show that the *rate* of increase of mechanical integrity of a fresh fracture can be significantly enhanced using electromagnetically induced pulsating current. It is thus apparent that a pure electrical input (not achievable using electrodes) can be interpreted as information by the cell/tissue complex to modulate the rate of a key cellular step. At this time it is not possible to establish the exact mechanism of this approach at *both* the electrochemical and biochemical level. However, certain preliminary conclusions can be formulated concerning the electrochemical aspect. The original choice of waveform parameters was predicated upon the desire to kinetically couple to potential dependent processes at the cell surface, which were presumed to act as key steps in regulation and control. In order to quantitatively test this hypothesis, it was necessary to ascertain the following:

a. whether kinetic coupling could be achieved by utilizing waveforms having widely different parameters designed to test for both kinetic and reversibility factors.
b. whether a net perturbation or periodic stimulus with respect to basic cell cycles was required.
c. whether results from a and b could be utilized to establish a quantita-

tive correlation between overall waveform characteristics and modulation of biological end point.

Both a and b were addressed and answered by utilizing the waveforms shown in Figure 13-4. It is to be remembered that the variations in both opposite polarity configuration and basic pulse mode were designed to primarily test for the degree of nonlinearity present in the essential receptor process. Clearly, absolute linearity would result in no *net* effect; if this is required (as asked in b), then correlations would be expected commensurate with the individual relaxation times involved. In actual fact, the answer to c strongly indicates that net effects are most relevant as is expected for processes that fall into the catalytic-type category. For example, if either the number of ion binding sites of membrane-bound enzyme or binding kinetics are altered over time due to irreversibility, activity changes could occur resulting in a net increase (decrease) in a biological end point that is catalyzed by the perturbed surface process.

The preliminary results obtained in this study clearly point the way for the use of this fracture model to assess the effect of signal parameters; to search for both electrical and biological dose "windows"; and to test programmation for optimal electrochemical-biochemical coupling as tissue differentiation proceeds. Parallel studies at the cellular level in a variety of systems show that the electrochemical information transfer concept appears to be a general one. It is intriguing to speculate that the cell surface processes common to all systems may be those regulating active transport. Electrochemical coupling to the cell surface portion of these processes could well be a generalized mode by which weak pulsating currents can modulate cell function.

REFERENCES

1. Bassett, C. A. L.; Pilla, A. A.; and Pawluk, R. J.: *Clin. Orthop., 124:*117, 1977.
2. Burr, H. S. and Hovland, C. I.: *Yale J. Biol. Med., 9:*541, 1937.
3. Pilla, A. A.: Proc. 7th Intersoc. Energy Conv. and Engineering Conf., Amer. Chem. Soc., Washington, D.C., 1972, p. 761.
4. Pilla, A. A.: *Ann. N.Y. Acad. Sci. 238:*149, 1974.
5. Pilla, A. A.: In Brighton, C. T., ed., *Electric and Magnetic Control of Musculoskeletal Growth and Repair,* New York, Grune and Stratton, 1979.
6. Barth, L. G. and Barth, L. J.: *Develop. Biol. 20:*269, 1969.
7. Pilla, A. A.: *Bioelectrochem. and Bioenergetics, 1:*227, 1974.
8. Smith, S. D.; Thomas, C. L.; and Frash, S. F.: *Bioelectrochem. and Bioenergetics 5:*177, 1978.
9. Chiabrera, A.; Hisenkamp,M.; Pilla, A. A.; Ryaby, J.; Ponta, D.; and Nicolini, C.: *J. Histochem. and Cytochem.,* 27:375, 1979.
10. Bassett, C. A. L.; Becker, R. O.; and Pawluk, R. J.: *Nature, 204:*652, 1964.
11. Brighton, C. T.; Cronkey, J. E.; and Osterman, A. L.: J. Bone and Joint Surg. 58A:368, 1975.
12. Zengo, A. N., Bassett, C. A.; and Prountzos, G.: *J. Dental Res. 55:*383, 1976.

13. Becker, R. O. and Spadaro, J. A.: *J. Bone and Joint Surg., 60A*:871, 1978.
14. Rodan, G. A.; Bourrett, L. A.; and Norton, L. A.: *Science, 137*:1063, 1962.
15. Bassett, C. A. L. and Becker, R. O.: *Science, 137*:1063, 1962.
16. Cochran, G. V. B.; Pawluk, R. J.; and Bassett, C. A. L.: *Clin. Orthop. 58*:249, 1968.
17. Black, J. and Korostoff, E.: *Ann. N.Y. Acad. Sci. 238*:95, 1974.
18. Marino, A. and Becker, R. O.: *Calc. Tiss. Res., 14*:327, 1974.
19. Fukada, E. and Yasuda, I.: *J. Physical Soc. (Japan), 12*:1158, 1957.
20. Pilla, A. A. and Margules, G. S.: *J. Electrochem. Soc., 124*:1697, 1977.
21. Bawin, S. M.; Adey, W. R.; and Sabbot, I. M.: *Proc. Natl. Acad. Sci. (U.S.A.), 75*:6314, 1978.
22. Pilla, A. A.: In *Proceedings, 1st U.S.-Australian Workshop on Bioelectrochemistry*, H. Keyser, ed. New York, Plenum, 1980a.
23. Pilla, A. A: In Brighton, C. T.; Black, J.; and Pollack, S. R., eds., *Electrical Properties of Bone and Cartilage*. New York, Grune and Stratton, 1979, p. 455.
24. Bassett, C. A. L.; Mitchell, S.; Norton, L.; and Pilla, A. A.: *Acta Orthoped. Belg., 40*:706, 1978.
25. Bassett, C. A. L.; Mitchell, S. N.; Norton, L.; Caulo, N.; and Gaston, R. R.: In *Electrical Properties of Bone and Cartilage*. Brighton, C. T.: Black, J.; and Pollack, S. R., eds. New York, Grune and Stratton, 1979, p. 605.
26. Schmukler, R. and Pilla, A. A.: *J. Electrochem. Soc., 127*:130C, 1980.
27. Pilla, A. A.: *Adv. in Chem. 188*:126, 1980.
28. Pilla, A. A. and Colacicco, G.: *J. Electrochem. Soc., 127*:129C, 1980.